https://doi.org/10.5194/tc-2021-134
Preprint. Discussion started: 17 June 2021

The Cryosphere Discussions
Open Access
EGU

The sensitivity of landfast sea ice to atmospheric forcing in single-column model simulations: a case study at Zhongshan Station, Antarctica

Fengguan Gu[1], Qinghua Yang[1], Frank Kauker[2,3], Changwei Liu[1], Guanghua Hao[4], Chaoyuan Yang[1], Jiping Liu[5], Petra Heil[6], Xuewei Li[1], Bo Han[1*]

1 School of Atmospheric Sciences, Sun Yat-sen University, and Southern Marine Science and Engineering Guangdong Laboratory (Zhuhai), Zhuhai 519082, China

2 Alfred Wegener Institute, Helmholtz Centre for Polar and Marine Research, Am Handelshafen 12, 27570 Bremerhaven, Germany

3 Ocean Atmosphere Systems, Tewesstseg 4, 20249 Hamburg, Germany

4 Key Laboratory of Marine Hazards Forecasting, National Marine Environmental Forecasting Center, Ministry of Natural Resources, Beijing 100081, China

5 Department of Atmospheric and Environmental Sciences, State University of New York at Albany, Albany, NY, USA

6 Australian Antarctic Division and Australian Antarctic Program Partnership, Private Bag 80, Hobart, Tas 7001, Australia

Correspondence to: Bo Han (hanb5@mail.sysu.edu.cn)

Abstract

Single-column sea ice models are used to focus on the thermodynamic evolution of the ice. Generally these models are forced by atmospheric reanalysis in absence of atmospheric *in situ* observations. Here we assess the sea ice thickness (SIT) simulated by a single-column model (ICEPACK) with *in situ* observations obtained off Zhongshan Station for the austral winter of 2016. In the reanalysis the surface air temperature is about 1 °C lower, the total precipitation is about 2 mm day^{-1} larger, and the surface wind speed is about 2 m s^{-1} higher compared to the *in situ* observations, respectively. Using sensitivity experiments we evaluate the simulation bias in sea ice thickness due to the uncertainty in the individual atmospheric forcing variables. We show that the unrealistic precipitation in the reanalysis leads to a bias of 14.5 cm in sea ice thickness and of 17.3 cm in snow depth. In addition, our data show that increasing snow depth works to gradually inhibits

https://doi.org/10.5194/tc-2021-134
Preprint. Discussion started: 17 June 2021

the growth of sea ice associated with thermal blanketing by the snow due to changing the vertical heat flux. Conversely, given suitable conditions, the sea ice thickness may grow suddenly when the snow load gives rise to flooding and leads to snow-ice formation. A potential mechanism to explain the different characteristics of the precipitation bias on snow and sea ice is discussed. The flooding process for landfast sea ice might cause different effect compared to pack ice, thus need to be reconsidered in ICEPACK. Meanwhile, the overestimation in surface wind speed in reanalysis is likely responsible for the underestimation in simulated snow depth, however this had little influence on the modelled ice thickness.

1 Introduction

Sea ice plays an important role in the global climate system by reflecting solar radiation and regulating the heat, moisture and gas exchanges between the ocean and the atmosphere. In contrast to the rapid decline of sea ice extent and volume in the Arctic (Stroeve et al., 2012; Lindsay and Schweiger, 2015), satellite observations show a slight increase in the yearly-mean area of Antarctic sea ice since the late 1970s (Parkinson and Cavalieri, 2012) followed by a rapid decline from 2014 (Parkinson, 2019) and a renewed increase in most recent years (Chemke and Polvani, 2020). Although the sudden decline of Antarctic sea ice is yet to be attributed (Parkinson, 2019), the spatial pattern of Antarctic sea ice changes is suggested to be largely caused by changes in the atmospheric forcing. For example, the rapid ice retreat in the Weddell Sea from 2015 to 2017 has been associated with the intensification of northerly wind (Turner et al., 2017), while the phase of the southern annular mode (SAM) significantly modulates the sea ice in Ross Sea and elsewhere, especially in November 2016 (Stuecker et al., 2017; Schlosser et al., 2018; Wang et al., 2019a).

Landfast sea ice, the immobile fraction of the sea ice, is mainly located in near coastal regions of Antarctica and its change is assumed to be indicative for the evolution of total Antarctic sea ice (Heil et al., 1996; Heil, 2006; Lei et al., 2010; Yang et al., 2016a). Different from drifting sea ice, the change in landfast sea ice is dominated by thermodynamic processes which can be simulated by single-column sea ice models (Heil et al., 1996; Lei et al., 2010; Yang et al., 2016b; Zhao et al., 2017). Furthermore, a single-column sea ice model is a useful tool to evaluate the impacts of different atmospheric forcings on the sea ice evolution because of the relatively simple structure of the physical processes (Cheng et al., 2013; Wang et al., 2019b; Merkouriadi et al., 2020). In this

https://doi.org/10.5194/tc-2021-134
Preprint. Discussion started: 17 June 2021

study, a state of the art single-column sea ice model, ICEPACK, is chosen to investigate the sensitivity of landfast sea ice to atmospheric forcing for the region off Zhongshan Station in Prydz Bay, East Antarctica (Figure 1).

Due to the lack of *in situ* observation, the majority of sea ice studies, especially for the Antarctic, rely on numerical models. Whether the model is under realistic atmospheric forcing is essential for the simulation results. Although being criticized for large deviations from *in situ* observations (Bromwich et al., 2007; Vancoppenolle et al., 2011; Wang et al., 2016; Barthélemy et al., 2018), atmospheric reanalysis data are assumed to offer reasonable atmospheric forcing for large-scale sea ice models for the Antarctic (Zhang, 2007; Massonnet et al., 2011; Zhang, 2014; Barthélemy et al., 2018). Previous studies reported a large spread between four global atmospheric reanalysis products and *in situ* observations in the Amundsen Sea Embayment (Jones et al., 2016). Moreover, studies showed that directly using atmospheric reanalyses as forcing for models causes significant biases in the Arctic sea ice simulations (Lindsay et al., 2014; Wang et al., 2019b). Similar results, accentuated by the sparseness at atmospheric observations entering the reanalysis, can be foreseen for Antarctica. Therefore, before simulating Antarctic sea ice the atmospheric forcing needs to be evaluated carefully. To our knowledge, few studies have given a quantitative evaluation on the effect of different atmospheric forcing on sea ice simulations in Antarctica.

The coastal landfast sea ice in Prydz Bay is generally first-year ice. It usually fractures and is exported or melts out completely between December and the following February and refreeze occurs from late February onwards (Lei et al., 2010). This seasonal cycle is representative of Antarctic landfast sea ice. In this study, we are aiming to evaluate the contributions of the various atmospheric forcing variables on landfast sea ice growth. The snow cover exerts influence on evolution of the vertical sea ice-snow column via a number of mechanisms, including the formation of snow-ice aided by flooding (Leppäranta, 1983). Understanding the snow depth is a major concern here. This study is arranged as follow: In section 2 the employed *in situ* observations, the numerical model and the reanalysis are introduced. The main results are given in section 3 focusing on the effect of different kinds of atmospheric forcing on sea ice and snow. Discussion and conclusions follow in sections 4 and 5.

https://doi.org/10.5194/tc-2021-134
Preprint. Discussion started: 17 June 2021

2 Materials and methods

2.1 Meteorological observation

The site of sea ice observation is in the coastal area off Zhongshan Station [(69◦22′S,76◦22′E); Figure 1], East Antarctica. The meteorological data were collected at a year-round manned weather observatory run at Zhongshan Station in 2016, which is 1 km inland from the sea ice observation site and 15 m above sea level. Snow fall is measured every 12 hours at the Russian Progress II station (located ~1 km to the southeast of Zhongshan Station). Other meteorological variables are available as hourly data, including 2m air temperature (T_{2m}), surface pressure (P_a), specific humidity (calculated from dew-point temperature and P_a), potential temperature (calculated from T_{2m} and P_a), air density (calculated by T_{2m} and P_a) and 10m wind speed (U_{10}) (Hao et al., 2019; Hao et al., 2020; Liu et al., 2020).

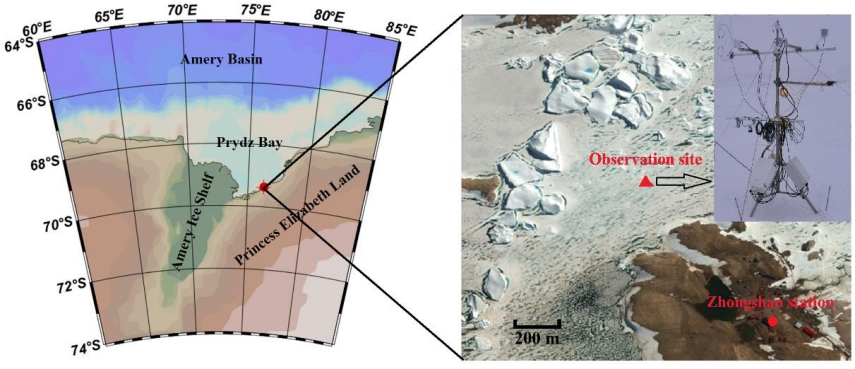

Figure 1 Location of landfast sea ice surface measurements near Zhongshan Station. The solid triangle denotes the observation site, the solid circle marks Zhongshan Station.

The short- and long-wave radiation were measured with a net radiometer mounted 1.5 m above the surface on a tripod. The net radiometer includes a pyranometer and a pyrgeometer. The pyranometer measures incoming and outgoing shortwave radiation and the pyrgeometer measures downward and upward longwave radiation. The spectral range of the pyranometer is 310–2800 nm, while the spectral range of the pyrgeometer is 4500–42000 nm. The uncertainty associated with the radiation measurements is ±5% (Yang et al., 2016a).

2.2 Sea ice thickness measurement

A thermistor-chain unit developed by Taiyuan University of Technology (TY) was used to

https://doi.org/10.5194/tc-2021-134
Preprint. Discussion started: 17 June 2021

measure sea ice thickness in austral winter 2016. This unit is composed of two parts: the control unit and the thermistor chain. The controller initiates data acquisitions, and records and stores the temperature measurements. The thermistor chain is 3 m long with 250 equidistant thermistors. Their sensitivity is 0.063 °C, and the measurement accuracy is better than ±0.5 °C. The thermistor chain records the vertical temperature profile across the near-surface atmosphere, any snow cover, the sea ice and the surface sea water simultaneously. Measurements are hourly. Details about the instruments are given in Hao et al. (2019).

Snow thickness close to the thermistor unit is measured weekly using a ruler with an accuracy of ±0.2 cm. Sea ice thickness is measured with ruler through a drill hole (5 cm diameter) weekly, the measurement accuracy is ±0.5 cm. The average thickness obtained from three close-by sites is retained. The measurement accuracy of ice thickness is ±0.5 cm. Sea-surface temperature and sea-surface salinity are measured in the drill holes weekly using a Cond 3210 set 1 (Hao et al., 2019). For both, the average temperature across three drill holes is recorded.

2.3 Atmospheric reanalysis data

The European Centre for Medium-range Weather Forecasts (ECMWF) released ERA5, the new reanalysis product in 2017 which is updated in near real-time (Hersbach and Dee, 2016; Hersbach et al., 2020). The complete ERA5 dataset, extending back to 1950, has been available to the end of 2019 during this study. Compared with the popular ERA-Interim reanalysis there are several major improvements in ERA5, including much higher resolutions (both, spatially and temporally). ERA5 has global coverage with a horizontal resolution of 31km by 31 km at the equator and 10km by 31km at the latitude of Zhongshan Station. In the vertical ERA5 resolves the atmosphere using 137 vertical pressure levels from the surface up to a geopotential height of 0.01 hPa. ERA5 provides hourly analysis and forecast fields and applies a four dimensional variational data assimilation system (4D-var). Data frequency is daily. ERA5 includes various reprocessed quality-controlled data sets, for example, the reprocessed version of the Ocean and Sea Ice Satellite Application Facilities (OSI SAF) sea ice concentration (Hersbach and Dee, 2016; Hersbach et al., 2020). For comparison and evaluation against observations in the Antarctic, ERA5 is interpolated to the observation site (described in 2.1).

2.4 ICEPACK

ICEPACK is a column-physics component of the Los Alamos Sea Ice Model (CICE) V6 and is

https://doi.org/10.5194/tc-2021-134
Preprint. Discussion started: 17 June 2021

maintained by the CICE Consortium. ICEPACK incorporates column-based physical processes that affect the area and thickness of sea ice. It includes several options for simulating sea ice thermodynamics, mechanical redistribution (ridging) and associated area and thickness changes. In addition, the model supports several tracers, including thickness, enthalpy, ice age, first-year ice area, deformed ice area and volume, melt ponds, and biogeochemistry (Hunke et al., 2019). ICEPACK Version 1.1.1 was used in this study and detailed options of physical parameterizations and model settings for the ICEPACK are summarized in Table 1. We employ ICEPACK to distribute the initial ice thickness to each ice thickness category using a distribution function:

$$p_i = \frac{max\left(2 \times h \times H_i - H_i^2, 0\right)}{\sum max\left(2 \times h \times H_i - H_i^2, 0\right)}, i = 1, N$$

Where, h is Initial ice thickness, H_i is the prescribed ice thickness category (0–0.6, 0.6–1.4, 1.4–2.4, 2.4–3.6, and above 3.6 m~; same as for Arctic simulations), N is the number of ice thickness category.

Table 1 Detailed options of physical parameterizations and model settings for the ICEPACK.

ICEPACK	Value
time step	3600 s
Number of layers in the ice	7
Number of layers in the snow	1
Ice thickness categories	5 (Bitz et al., 2001)
Initial ice thickness	98 cm
Initial snow depth	10 cm
Albedo scheme	CCSM3 (Collins et al., 2006)
Ice thermodynamic	Mushy-layer (Turner et al., 2013)
Shortwave radiation	Delta-Eddington (Briegleb and Light, 2007)

The atmospheric forcing for the ICEPACK model consists of observations of downward short- and longwave radiation, 2m air temperature, specific humidity, total precipitation, potential temperature, 2m air density, and 10m wind speed. The oceanic forcing includes sea surface temperature, sea surface salinity, and oceanic mixed layer depth. The period concerned in this study is from 22 April, when observed sea ice generally starts to grow, to 22 November in 2016. Since there are no observations of the ocean mixed-layer depth, we set it to 20 m (default in ICEPACK).

Two sets of atmospheric forcing have been chosen. The first is spatially interpolated ERA5 onto the location of the observation site, and the second is using *in situ* atmospheric observations. It is

https://doi.org/10.5194/tc-2021-134
Preprint. Discussion started: 17 June 2021

well-known that the simulation biases of numerical models are introduced through many shortcomings including unrealistic surface boundary conditions (here: atmospheric forcing), imperfect physical process formulations, computational errors, etc. Understanding the uncertainty in sea ice simulations as well as the sea ice response pattern in climate change scenario due to imperfect surface boundaries is a prerequisite for successful simulations and needs to be assessed first.

3 Results

3.1 Surface atmospheric conditions near the observation site

First we compare the eight atmospheric variables used to force ICEPACK (surface downward shortwave radiation (R_{sd}), surface downward longwave radiation (R_{ld}), surface air temperature (T_a), specific humidity (Q_a), precipitation (P), air potential temperature (Θ_a), air density (ρ_a), wind speed (U_a) with the respective *in situ* observation. Table 2 lists the bias (simulation minus observation), the mean value of the *in situ* observation (Mean_Obs), the correlation coefficient (Corr.) and the root-mean-square deviation (RMSD) between the interpolated ERA5 data and the observation. In general, all eight variables from the two sources follow each other quite closely (correlation coefficients between ERA5 and the observations greater than 0.85), except for P and U_a. These variables exhibit the largest relative deviations (in bias and absolute magnitude). Previous studies have shown that across the atmospheric forcing variables, uncertainties in T_a, P, and U_a exert significantly influence the sea ice thickness (Cheng et al., 2008), while surface wind may affect the snow cover in two ways: 1) sublimation can strongly reduce the snow cover in dry air and strong wind condition (Gascoin et al., 2013), 2) surface wind can modulate latent and sensible heat flux in the bulk formation (Fairall et al., 2003). In this study, main attention is paid on these three atmospheric variables.

The timing of daily variations of T_a are well represented by ERA5, especially for strong cooling events (Figure 2a). However, ERA5 tends to underestimate warm events by a few degree as well as cold events where differences exceeding 10 °C may occur (Figure 2d). During the entire observation period in 2016, T_a from ERA5 was 1.168 °C lower than in the *in situ* observation. Also previous studies reported similar disagreement in T_a between observation and reanalysis in Antarctica. The cold bias of T_a in the reanalysis was suggested to be caused by the ice surface schemes that can not

https://doi.org/10.5194/tc-2021-134
Preprint. Discussion started: 17 June 2021

196 accurately describe the ice-atmosphere interactions of strongly stable stratified boundary layers that
197 are frequent in Antarctica (Bracegirdle and Marshall, 2012; Fréville et al., 2014).
198
199 Table 2 Comparison of atmospheric forcing between ERA5 reanalysis and *in situ* observations.

Variable	Bias	Mean_Obs	Corr	RMSD
R_{sd} (W m^{-2})	6.115	67.714	0.967	40.981
R_{ld} (W m^{-2})	-19.153	198.023	0.869	28.753
T_a (K)	-1.168	-15.340	0.967	2.820
Q_a (10^{-4} kg kg^{-1})	-0.769	8.247	0.950	1.987
P (mm day^{-1})	2.010	0.660	0.639	0.825
Θ_a (K)	0.290	-13.712	0.965	2.609
ρ_a (kg m^{-3})	-0.021	1.322	0.958	0.026
U_a (m s^{-1})	2.145	4.228	0.765	2.989

200
201 The reanalyzed variable with the largest deviation from the observation is the precipitation
202 (Figure 2b). Hourly precipitation from ERA5 was accumulated into daily data and compared with
203 the daily precipitation records from the Progress II station. The maximum daily mean precipitation
204 can reach 19.1 mm day^{-1} (11 July 2016) with an average precipitation of 0.66 mm day^{-1} from April
205 29 to November 22, 2016. While ERA5 captures the main precipitation events, it significantly
206 overestimated the magnitude of precipitation events, especially in July. In this month, the mean
207 precipitation rate from ERA5 is 5.83 mm day^{-1}, while observed is only 1.42 mm day^{-1}. From April
208 to November, the accumulated precipitation from ERA5 is about 300% larger than that in the *in situ*
209 observations. Nevertheless, using precipitation from Russia's Progress II for Zhongshan Station may
210 be questioned as well because of the distance of 1km to Zhongshan Station. Moreover, a given
211 precipitation rate (snow fall) might cause a range of snow cover patterns because the snowdrift is
212 quite strong and responsible for the larger deviation (Liston et al., 2018).
213
214

https://doi.org/10.5194/tc-2021-134
Preprint. Discussion started: 17 June 2021

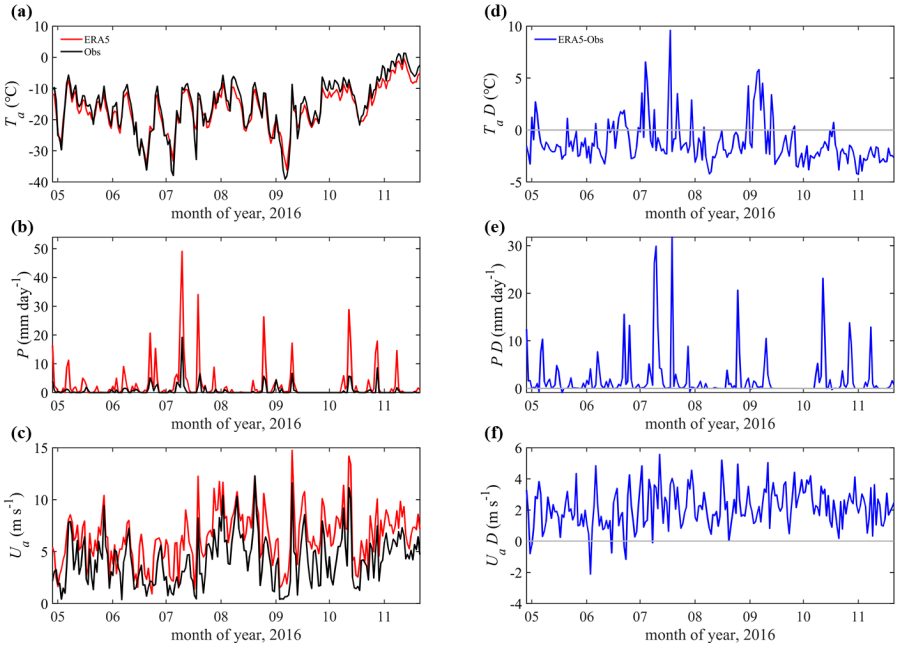

Figure 2 Time series of daily (a) surface air temperature, (b) precipitation rate, and (c) wind speed (10 m above the surface). The ERA5 reanalysis data are indicated as red lines. Observations are marked by black lines. (d-f) show the difference (marked by '*D* ') between ERA5 and the observation (ERA5-observation). The differences are marked by blue lines. The gray lines denote the zero line.

The wind speed observation varied from 0.01 m s^{-1} to 12.3 m s^{-1} with an average 4.2 m s^{-1} and with maxima in August. ERA5 well captured the timing of strong wind events but overestimated the magnitude of daily surface wind on average by 2.1 m s^{-1}. One potential cause of the overestimation is that the numerical model underlying ERA5 cannot represent the roughness correctly due to the complex orography (Tetzner et al., 2019) and the effect of katabatic wind regions (Vignon et al., 2019).

3.2 Simulation forced by observed *in situ* atmospheric variables

The simulation bias of sea ice thickness and snow depth is impacted by many aspects, including unrealistic atmospheric and oceanic forcing and shortcomings in the applied numerical model. In this study, we mainly focus on the influence of imperfect atmospheric forcing.

The sea ice thickness measured through a hole drilled by an ice auger (5cm in diameter) is

https://doi.org/10.5194/tc-2021-134
Preprint. Discussion started: 17 June 2021

232 increasing from 29 April (100±2 cm) to 25 October (172±2cm), remaining level from there on
233 (Figure 3a). The ice thickness deduced from the TY thermistor-chain buoy shows a similar result:
234 sea ice thickness increasing from 106 cm on 22 April to 171 cm on 17 November. In November the
235 sea ice thickness is stationary, indicating a thermodynamic equilibrium between heat loss to the
236 atmosphere and heat gain from the ocean (Yang et al., 2016a; Hao et al., 2019).

237 When forced by atmospheric i*n situ* observations, the simulated sea ice thickness agrees well
238 with the observed thickness with a mean bias of less than 1 cm over the growth season. We attribute
239 the good simulation result to the fact that seasonal evolution of landfast is largely driven by thermal
240 processes which ICEPACK captures well using *in situ* forcing.

241 The average observed snow depth during the ice-growth season is 17cm with low snow depth
242 measured prior to 11 July. Thereafter, the snow depth increases rapidly up to about 37cm associated
243 with a precipitation event arising from a single synoptic system. It then decreases to below the
244 seasonal mean, only to obtain two secondary maxima in snow depth (about 25cm) on 2 August and
245 8 September. The simulated snow depth tracks the observation closely before 2 August (Figure 3b).
246 Then, when the observed snow depth decreased quickly from about 30 cm to about 10 cm, while
247 the simulation continues to increase gradually until the onset of surface melting in November. We
248 attribute the observed quick decrease of snow depth to the effect of snowdrift, because the surface
249 wind stayed above 5 m s^{-1} for most of August (Figure 2c), giving rise to snow drift, a process not
250 implemented in the version of ICEPACK used here.

251 Using observed meteorological variables as atmospheric forcing in ICEPACK produce
252 unreliable snow depth while the sea ice thickness was in reasonably good agreement. In other words,
253 the large bias in snow depth seems to have little effect on the sea ice thickness in the simulation.
254 This counter-intuitive finding is of great interest to us because the snow layer is crucial in
255 modulating the energy exchange on top of the sea ice. Potential causes of for this result will be
256 discussed later.
257

https://doi.org/10.5194/tc-2021-134
Preprint. Discussion started: 17 June 2021

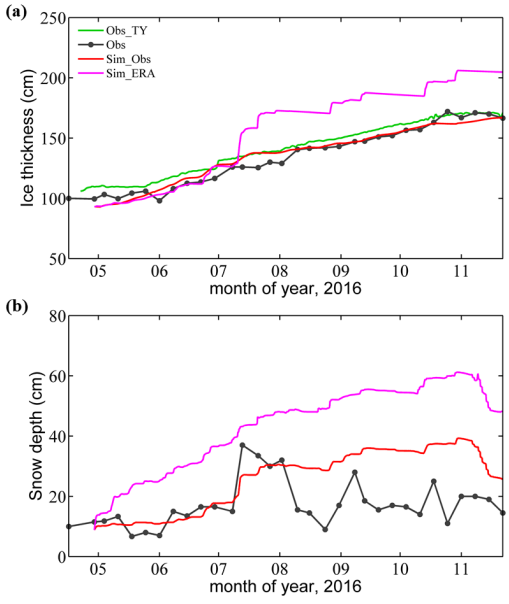

Figure 3 Time series of (a) sea ice thickness and (b) snow depth during the freezing season. Black solid lines with black point show the observations from the drill hole (Obs). Green solid lines show the ice thickness derived from the TY buoy (Obs_TY). Red solid lines show the simulation results under *in situ* atmospheric forcing (Sim_Obs) and magenta solid lines are simulation result under ERA5 forcing (Sim_ERA).

3.3 Simulation forced by ERA5 atmospheric variables

When forced by ERA5, the simulation shows much greater deviations in ice thickness (Figure 3a). Simulated sea ice thickness is close to the observation before 11 July with only a small positive bias of about 1 cm. However, from 11 July to November, the mean bias becomes about 33 cm. During this period, a sudden increase in sea ice thickness happens on 11 July. Thereafter, the offset in the sea ice thickness between the simulation and the observation remains almost constant.

In contrast to the simulated sea ice thickness, the simulated snow depth is much greater than observed even before 11 July. Near the extremely large precipitation event (~19 mm day^{-1}) in July 11 (Figure 2b), the observed snow depth increases from <20 cm to about 40 cm. Although the precipitation rate from ERA5 is more than 2 times larger as observed on July 11 (~40 mm day^{-1}) the event is almost not visible in the simulated snow depth. The snow depth increase is near linear from about 10cm at time of model initiation to almost 60cm at the onset of surface melting in November.

https://doi.org/10.5194/tc-2021-134
Preprint. Discussion started: 17 June 2021

For the entire simulation period, the precipitation from ERA5 obviously causes an overestimation in snow depth.

3.4 Sensitivity simulations

To find out which atmospheric variables including T_a, P and U_a are the most crucial in the sea ice simulation, a set of sensitivity simulation experiments is conducted, named SEN1. The simulation under the forcing from the *in situ* observed atmospheric variables is the control experiment and named Sim_Obs. In each experiment of SEN1, one atmospheric variable is replaced by the corresponding variable from ERA5 while all others are identical to those of the control experiment. In Table 3, the averaged bias between the simulation and the observation of the outputs (ice thickness and snow depth) or the forcing atmospheric variable, are listed separately.

Table 3 Bias of ice thickness, snow depth and each forcing variables derived from SEN1. 'All' means using the full set of ERA5 atmospheric forcing

Variable	Bias		
	Ice (cm)	Snow (cm)	Forcing
R_{sd} (W m^{-2})	-0,044	-0.130	6.115
R_{ld} (W m^{-2})	3.050	2.243	-19.153
T_a (K)	0.001	0.029	-1.168
Q_a (10^{-4} kg kg^{-1})	1.099	-1.299	-0.769
P (mm day^{-1})	14.519	17.312	2.01
Θ_a (K)	-0.483	0.407	0.290
ρ_a (kg m^{-3})	0.119	-0.071	-0.021
U_a (m s^{-1})	-0.311	-3.421	2.145
All	16.824	17.882	/

Comparing the individual biases, it turns out that P, R_{ld} and Q_a from ERA5 contribute to the bias in sea ice thickness most strongly. For snow depth P, U_a and R_{ld} contribute largest. Note, that P and U_a from ERA 5 exhibits the largest bias with respect to the *in situ* observation. It can also be seen that sea ice thickness and snow depth are impacted strongly by the biases in R_{ld} and Q_a. In contrast, T_a from ERA5 is close to the *in situ* observation, so the simulated sea ice thickness and snow depth is hardly impacted. The results from SEN1 reveal that the overestimation in P in ERA5 is the major source for the overestimation of sea ice thickness and snow depth and that the overestimation in U_a partly neutralizes the overestimation in snow depth. For convenience, the simulation with only one

https://doi.org/10.5194/tc-2021-134
Preprint. Discussion started: 17 June 2021

atmospheric variable (X) replaced by the corresponding ERA5 variable is named SIM_ERA_X.

Compared with Sim_Obs, Sim_ERA_P is overestimating the snow depth since May (Figure 4b) and shows a significant positive bias in sea ice thickness after 11 July. Before 11 July, the sea ice thickness from Sim_ERA_P was even smaller than from Sim_Obs (Figure 4a).

To find out why the snow and sea ice behave differently, we investigate the net heat flux into the ice surface H_N (positive downward):

$$H_N = Rn + Hs + Hl,$$

where Rn, Hs, and Hl are the net surface radiation flux, the sensible heat flux, and the latent heat flux, respectively. All energy fluxes are defined positive downward. Because the simulated snow layer in SIM_ERA_P is much deeper than in SIM_Obs, the difference of H_N reflects the modification of the surface energy flux due to the changed snow layer. From Figure 4c, it can be deduced that the overestimation of snow depth in SIM_ERA_P results in a positive anomaly of H_N before July 11, which hampers the sea ice growth. Later the difference of H_N becomes quite small. The dependence of H_N on the snow depth is significant when the snow layer is shallow (<20 cm in this study). If the snow layer is deep enough its impact on the net surface heat flux ceases.

After July 11, the difference in sea ice thickness between the two simulations increases quickly from ~0 to >40 cm (Figure 4a). We attribute that to flooding with subsequent snow-ice formation (Powell and others, 2005). The continuously deepening snow layer reduces the sea ice freeboard. When there is heavy snow fall, which happens frequently after July 11, the heave snow load subpresses the upper sea ice surface below sea level and sea water is flooding onto the sea ice surface causing the overlaying snow to freeze. This process increases the sea ice thickness rapidly (Figure 4d). The difference (~100 cm) in accumulated flooding ice (Figure 4b) is greater than the difference (~40 cm) in simulated sea ice thickness (Figure 4a), when the net surface heat flux over the sea ice seems to be close after July 11 (Figure 4d). We guess the reason for this difference may be that as the snow-ice process occurs, the increase in sea ice thickness will reduce the heat transfer between the ocean and the atmosphere, and inhibit the basal growth of sea ice in winter (Figure 4c). The flooding induced snow-ice formation happens with a rate larger than 0.5 cm per hour after July 11. Comparing Figure 4e with Figure 4f, we find that the change in snow depth is much lower than the accumulated snow fall because of flooding.

https://doi.org/10.5194/tc-2021-134
Preprint. Discussion started: 17 June 2021

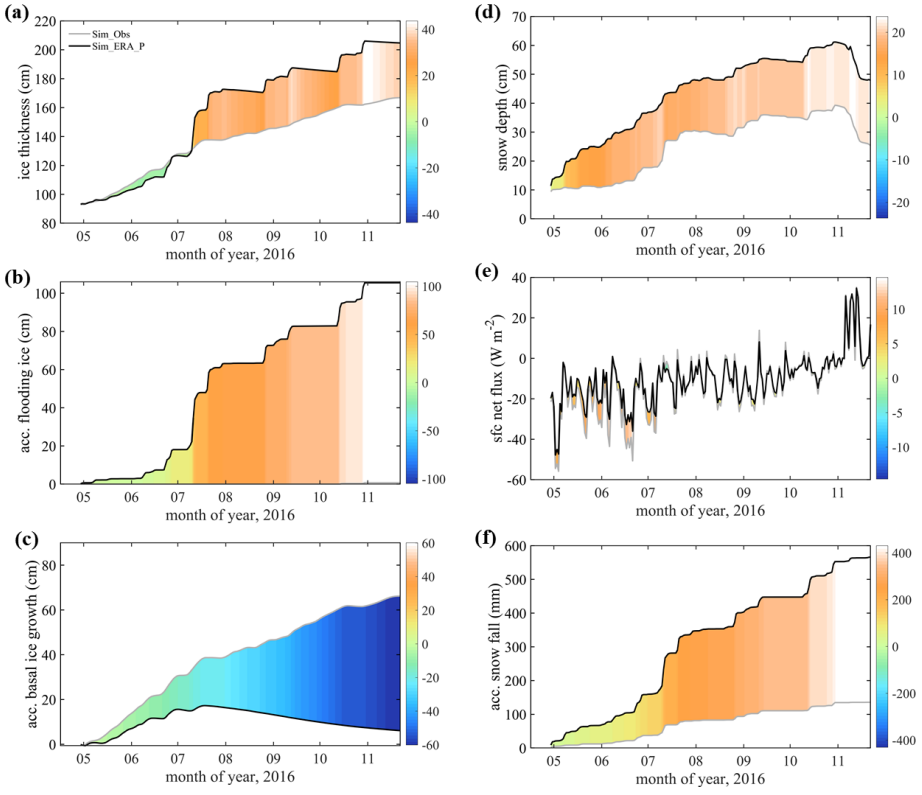

Figure 4 Times series of (a) sea ice thickness, (b) accumulated flooding ice, (c) accumulated basal ice growth, (d) net surface heat flux, (e) snow depth, and (f) accumulated snow fall. The gray line represents the simulation using precipitation from observation (Sim_Obs). The black line represents the simulation using precipitation from ERA5 (Sim_ERA_P). The color bar represents their difference (Sim_ERA_P – Sim_Obs).

https://doi.org/10.5194/tc-2021-134
Preprint. Discussion started: 17 June 2021

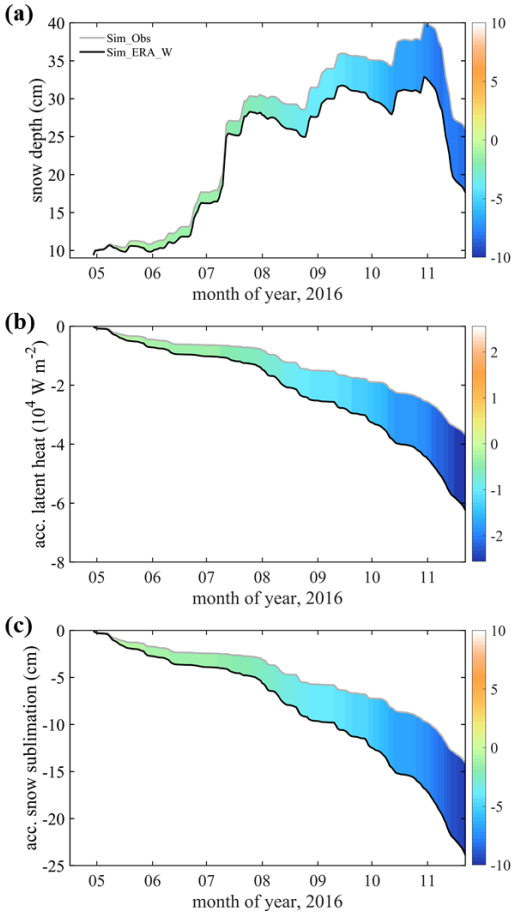

Figure 5 Times series of (a) snow depth, (b) accumulated latent heat flux and (c) accumulated snow sublimation. The gray line represents the simulation using wind from the observation (Sim_Obs). The black line represents the simulation using wind from ERA5 (Sim_ERA_W). The color bar represents their difference (Sim_ERA_W – Sim_Obs).

Although the snow-drift process is currently not implemented in ICEPACK, U_a still affects the snow depth through modifying the surface heat fluxes in the bulk formulations (Fairall et al., 2003). Compared with Sim_Obs, using U_a from ERA5 causes in the mean a by -5.1 W m^{-2} lower latent heat flux (Figure 5b), i.e. larger sublimation (Figure 5c), and a reduction of about -3.4 cm in the snow depth (Figure 5a). Therefore, when ERA5 is forcing ICEPACK, the overestimation in U_a partly neutralizes the effect of overestimation in P in ICEPACK at Zhongshan Station.

https://doi.org/10.5194/tc-2021-134
Preprint. Discussion started: 17 June 2021

346 **3.5 Additional Sensitivity simulations on the precipitation bias**

347 The precipitation from ERA5 not only shows the largest deviation compared to the *in situ*
348 observation, but also contributes largest to the bias in the sea ice and snow simulation. To find out
349 how sensitive sea ice and snow are on precipitation, 10 sensitivity experiments are set up, named
350 SEN2. In the *n*-th experiment, $n \times 10\%$ of the daily difference between *P* from ERA5 and the *in situ*
351 observation is added to the *in situ* observation on that day. This procedure increases the magnitude
352 of the precipitation gradually in the experiments, while the timing of the daily precipitation events
353 remains almost unchanged.
354

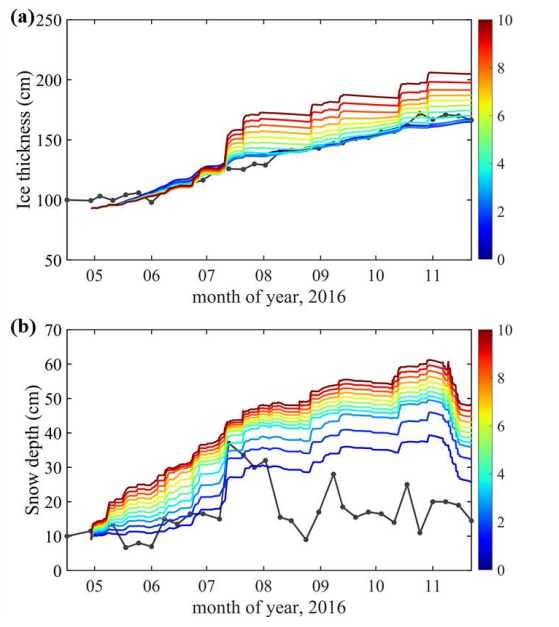

355

356 Figure 6 Time series of the simulated (a) sea ice thickness and (b) snow depth in the n experiments
357 of SEN2. The black solid line with black points show the *in situ* observations (Obs). The 11 colored
358 lines denote the 11 sensitivity experiments. When $n = 0$, precipitation is from the *in situ* observation.
359 When $n = 10$, precipitation is from ERA5.
360
361

https://doi.org/10.5194/tc-2021-134
Preprint. Discussion started: 17 June 2021

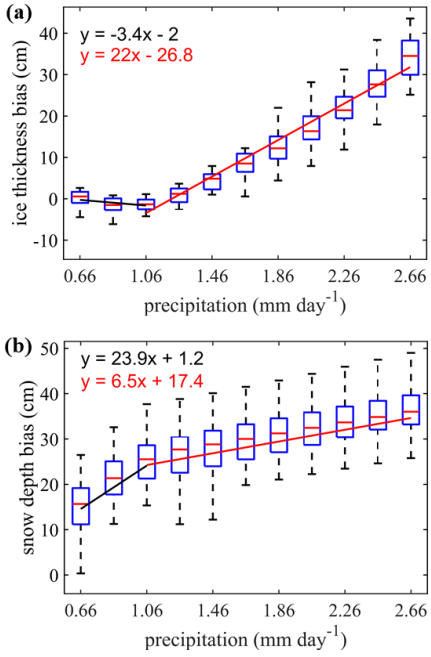

Figure 7 Box plot of simulation bias (simulation minus observation) of (a) sea ice thickness and (b) snow depth over the daily mean precipitation in the different sensitivity experiments (n increases from left to right). On the x-axis, 0.66 mm is referring to the experiment with n=0 (*in situ* precipitation) and 2.66 mm is referring to the n=10 experiment (ERA5 precipitation). Two linear regression lines (black and red) are derived for x <= 1.06 mm and x > 1.06 mm based on the mean of ice thickness and snow depth.

Both, sea ice thickness and snow depth exhibit a linear increase with increasing precipitation. The period we calculated the bias between simulations and observations was from 27 July to the end of November. Different start or end dates of this period do not change this result.

The simulation bias of the sea ice thickness is quite small before the precipitation increases by about 1 mm per day (Figure 7). In fact, the simulated sea ice thickness even decreases at a rate of -3.4 cm per 1 mm increase in precipitation. The stronger isolation of the snow layer hampers the sea ice growths. If precipitation is larger than 1 mm day^{-1}, an increase of 1 mm day^{-1} in precipitation is thickening the sea ice at the end of the simulation by 22cm. In contrast, an increase of 1 mm day^{-1} in precipitation is thickening the snow depth at the end of the simulation by 23.9cm when the enforced precipitation remains small, and by 6.5 cm when the added precipitation is large. These

https://doi.org/10.5194/tc-2021-134
Preprint. Discussion started: 17 June 2021

379 different effects of increases in precipitation on the snow and sea ice growth is illustrated in Figure
380 8 emphasizing the role of flooding via snow-ice formation.
381

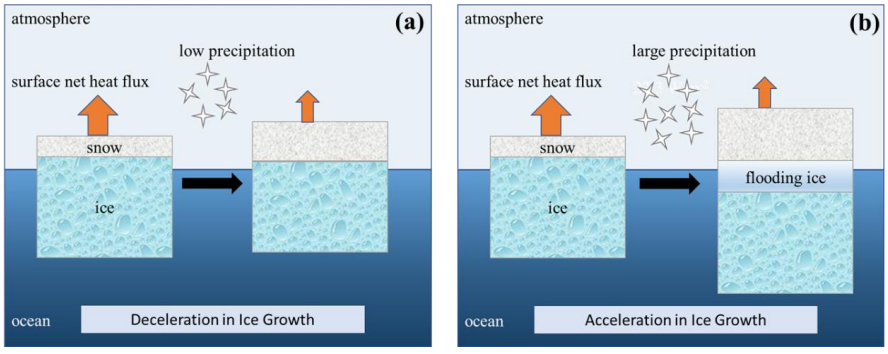

382
383 Figure 8 Schematic diagram for (a) low precipitation and (b) large precipitation illustrating
384 precipitation effects on sea ice growth. The upward arrow represents surface net heat flux.
385

386 **4 Discussions**

387 Rapid changes in snow depth can increase sea ice thickness through the formation of snow-ice
388 (Leppäranta, 1983) and superimposed ice (Kawamura et al., 1997). Superimposed ice usually
389 corresponds to liquid precipitation or melted snow permeate downward in the ice surface to form a
390 fresh slush layer that refreezes to form superimposed ice. Superimposed ice is significant in early
391 autumn when snow starts to melt (Kawamura et al., 1997) and is a significantly contributing to sea
392 ice growth (up to 20% of mass) (Granskog et al., 2004). The superimposed ice which is implemented
393 in ICEPACK with melt pond parametrization is not run in this study. Therefore, the simulation may
394 underestimate sea ice thickness and overestimate snow depth and we will apply the melt pond in the
395 follow-up research work.

396 Flooding induced snow-ice formation is a very important process in the Antarctic because of
397 thin ice and heavy snowfall (Kawamura et al., 1997). It can make a significant contribution to the
398 total ice mass (12%-36%) and reduces the snow cover by up to 42-70% of the total snow
399 accumulation depending on the season and location (Jeffries et al., 2001). However, snow-ice
400 formation might be overestimated on landfast sea ice when using ICEPACK, especially when ERA5
401 is taken as atmospheric forcing. Based on observations from a thermistor-chain buoy, a previous
402 study estimated that a slushy layer of 10cm depth will refreeze within 3 days (Provost et al., 2017).

https://doi.org/10.5194/tc-2021-134
Preprint. Discussion started: 17 June 2021

In ICEPACK, snow-ice can form at a fastest rate of 10 cm in 1 day.

Besides the atmospheric forcing, the ocean forcing also plays an important role on sea ice evolution. Heat flux from the ocean boundary layer modifies the sea ice energy balance (Maykut and Untersteiner, 1971). The ocean heat flux is mainly impacted by summer insolation through open leads, thin ice, and melt ponds (Perovich and Maykut, 1990) and upward transfer of heat through vertical turbulent mixing (McPhee et al., 1999). In this study, the oceanic forcing is determined by specifying the ocean temperature and salinity in an ocean mixed layer of 20m depth. Oceanic observations under sea ice are even more scarce than atmospheric observation over sea ice. Most sea ice models use empirical values or data from CCSM3 to set the ocean boundary values (e.g., Yang et al., 2016b; Turner and Hunke, 2015). However, just as the atmospheric forcing, the marine forcing needs to be evaluated carefully before using (e.g., Uotila et al., 2019).

5 Conclusions

In this work we use the single-column sea ice model ICEPACK forced by the ERA5 atmospheric reanalysis and by atmospheric *in situ* observations to simulate snow depth and sea ice thickness at Zhongshan Station, Antarctic. The main results are:

(1) Using atmospheric variables from *in situ* observations to force ICEPACK simulates the sea ice evolution well, but significantly overestimates the snow depth at Zhongshan Station.

(2) The average precipitation from ERA5 was about 2 mm day^{-1} greater than observed, hence producing a 14.5 cm excess in sea ice thickness and 17.3 cm more snow depth compared to the simulation forced by observed atmospheric variables. The large bias in precipitation is the main contributor to the simulation bias of sea ice thickness and snow depth between observations and model simulations.

(3) The mean surface wind speed from ERA5 is about 2 m s^{-1} higher than the observation. Directly using surface wind speed alone can reduce the snow bias by 3.4 cm. This is because the increase in latent heat accelerates snow sublimation, but has little effect on the sea ice thickness.

(4) The response of the sea ice thickness was found to depend on the snow depth. When the snow layer is shallow, the snow layer deepens quickly while the sea ice is even thinning slowly with increasing precipitation. The change in the surface net heat flux is suggested to be the dominant factor. While for a deeper snow layer, because the flooding process induces snow-ice formation, the

https://doi.org/10.5194/tc-2021-134
Preprint. Discussion started: 17 June 2021


The Cryosphere Discussions
Open Access
EGU

sea ice grows quickly while the snow depth increases only slowly. This study investigated the ERA5 reanalysis uncertainties and its impact on the sea ice simulation. In our future research, the ocean reanalysis errors and their impact on the sea ice simulation will be addressed as well. Furthermore, because the single-column model only considers sea ice thermodynamics, the full CICE sea ice model will be applied to conduct two dimensional numerical simulations of sea ice for the entire Southern Ocean to assess regional differences and to explore the underlying mechanisms.

Acknowledgments

The authors would like to thank ECMWF for the ERA5 reanalysis data set and the Russian meteorological station Progress II for the precipitation observations. We are grateful to CICE Consortium for sharing ICEPACK and its documentation (https://github.com/CICE-Consortium/Icepack). This study is supported by the National Natural Science Foundation of China (No. 41941009, 41922044), the Guangdong Basic and Applied Basic Research Foundation (No. 2020B1515020025), the Southern Marine Science and Engineering Guangdong Laboratory (Zhuhai) (No. SML2020SP007) and CAS "Light of West China" Program (No. E129030101, Y929641001). PH was supported by AAS grant 4506.

References:

Barthélemy, A., Goosse, H., Fichefet, T., and Lecomte, O.: On the sensitivity of Antarctic sea ice model biases to atmospheric forcing uncertainties, Clim. Dynam., 51, 1585-1603, 2018.

Bitz, C. M., Holland, M. M., Weaver, A. J., and Eby, M.: Simulating the ice‐thickness distribution in a coupled climate model, Journal of Geophysical Research: Oceans, 106, 2441-2463, 2001.

Bracegirdle, T. J., and Marshall, G. J.: The reliability of Antarctic tropospheric pressure and temperature in the latest global reanalyses, J. Climate, 25, 7138-7146, 2012.

Briegleb, B. P., and Light, B.: A Delta-Eddington multiple scattering parameterization for solar radiation in the sea ice component of the Community Climate System Model, NCAR Tech. Note NCAR/TN-472+STR, 1-108, 2007.

Bromwich, D. H., Fogt, R. L., Hodges, K. I., and Walsh, J. E.: A tropospheric assessment of the ERA‐40, NCEP, and JRA‐25 global reanalyses in the polar regions, Journal of Geophysical Research: Atmospheres, 112, D10111, 2007.

Chemke, R., and Polvani, L. M.: Using multiple large ensembles to elucidate the discrepancy between the 1979–2019 modeled and observed Antarctic sea ice trends, Geophys. Res. Lett., 47, e2020G-e88339G, 2020.

Cheng, B., Mäkynen, M., Similä, M., Rontu, L., and Vihma, T.: Modelling snow and ice thickness in the coastal Kara Sea, Russian Arctic, Ann. Glaciol., 54, 105-113, 2013.

Cheng, B., Zhang, Z., Vihma, T., Johansson, M., Bian, L., Li, Z., and Wu, H.: Model experiments on snow and ice thermodynamics in the Arctic Ocean with CHINARE 2003 data, Journal of Geophysical Research: Oceans, 113, C9020, 2008.

Collins, W. D., Bitz, C. M., Blackmon, M. L., Bonan, G. B., Bretherton, C. S., Carton, J. A., Chang, P., Doney, S. C., Hack, J. J., and Henderson, T. B.: The community climate system model version 3

https://doi.org/10.5194/tc-2021-134
Preprint. Discussion started: 17 June 2021

(CCSM3), J. Climate, 19, 2122-2143, 2006.
Fairall, C. W., Bradley, E. F., Hare, J. E., Grachev, A. A., and Edson, J. B.: Bulk parameterization of air–sea fluxes: Updates and verification for the COARE algorithm, J. Climate, 16, 571-591, 2003.
Fréville, H., Brun, E., Picard, G., Tatarinova, N., Arnaud, L., Lanconelli, C., Reijmer, C., and Van den Broeke, M.: Using MODIS land surface temperatures and the Crocus snow model to understand the warm bias of ERA-Interim reanalyses at the surface in Antarctica, The Cryosphere, 8, 1361-1373, 2014.
Gascoin, S., Lhermitte, S., Kinnard, C., Bortels, K., and Liston, G. E.: Wind effects on snow cover in Pascua-Lama, Dry Andes of Chile, Adv. Water Resour., 55, 25-39, 2013.
Granskog, M. A., Leppäranta, M., Kawamura, T., Ehn, J., and Shirasawa, K.: Seasonal development of the properties and composition of landfast sea ice in the Gulf of Finland, the Baltic Sea, Journal of Geophysical Research: Oceans, 109, 10.1029/2003JC001874, 2004.
Hao, G., Pirazzini, R., Yang, Q., Tian, Z., and Liu, C.: Spectral albedo of coastal landfast sea ice in Prydz Bay, Antarctica, J. Glaciol., 67, 1-11, 2020.
Hao, G., Yang, Q., Zhao, J., Deng, X., Yang, Y., Duan, P., Zhang, L., Li, C., and Cui, L.: Observation and analysis of landfast ice arounding Zhongshan Station, Antarctic in 2016, Haiyang Xuebao, 9, 26-39, 2019.
Heil, P.: Atmospheric conditions and fast ice at Davis, East Antarctica: A case study, Journal of Geophysical Research: Oceans, 111, C5009, 2006.
Heil, P., Allison, I., and Lytle, V. I.: Seasonal and interannual variations of the oceanic heat flux under a landfast Antarctic sea ice cover, Journal of Geophysical Research: Oceans, 101, 25741-25752, 1996.
Hersbach, H., Bell, B., Berrisford, P., Hirahara, S., Horányi, A., Muñoz Sabater, J., Nicolas, J., Peubey, C., Radu, R., and Schepers, D.: The ERA5 global reanalysis, Q. J. Roy. Meteor. Soc., 146, 1999-2049, 2020.
Hersbach, H., and Dee, D.: ERA5 reanalysis is in production, ECMWF Newsletter 147, Reading, UK: ECMWF. [Retrieved from https://www. ecmwf. int/en/newsletter/147/news/era5-reanalysis-production], 2016.
Hunke, E., Allard, R., Bailey, D. A., Blain, P., Craig, T., Dupont, F., DuVivier, A., Grumbine, R., Hebert, D., Holland, M., Jeffery, N., Lemieux, J., Rasmussen, T., Ribergaard, M., Roberts, A., Turner, M., and Winton, M.: CICE-Consortium/Icepack: Icepack1.1.1, doi:10.5281/zenodo.3251032, 2019.
Jeffries, M. O., Krouse, H. R., Hurst-Cushing, B., and Maksym, T.: Snow-ice accretion and snow-cover depletion on Antarctic first-year sea-ice floes, Ann. Glaciol., 33, 51-60, DOI: 10.3189/172756401781818266, 2001.
Jones, R. W., Renfrew, I. A., Orr, A., Webber, B., Holland, D. M., and Lazzara, M. A.: Evaluation of four global reanalysis products using in situ observations in the Amundsen Sea Embayment, Antarctica, Journal of Geophysical Research: Atmospheres, 121, 6240-6257, 2016.
Kawamura, T., Ohshima, K. I., Takizawa, T., and Ushio, S.: Physical, structural, and isotopic characteristics and growth processes of fast sea ice in Lützow-Holm Bay, Antarctica, Journal of Geophysical Research: Oceans, 102, 3345-3355, 10.1029/96JC03206, 1997.
Lei, R., Li, Z., Cheng, B., Zhang, Z., and Heil, P.: Annual cycle of landfast sea ice in Prydz Bay, east Antarctica, Journal of Geophysical Research: Oceans, 115, C2006, 2010.
Leppäranta, M.: A growth model for black ice, snow ice and snow thickness in subarctic basins, Hydrology Research, 14, 59-70, 1983.
Lindsay, R., Wensnahan, M., Schweiger, A., and Zhang, J.: Evaluation of seven different atmospheric reanalysis products in the Arctic, J. Climate, 27, 2588-2606, 2014.

https://doi.org/10.5194/tc-2021-134
Preprint. Discussion started: 17 June 2021

Lindsay, R., and Schweiger, A.: Arctic sea ice thickness loss determined using subsurface, aircraft, and satellite observations, The Cryosphere, 9, 269-283, 2015.

Liston, G. E., Polashenski, C., Rösel, A., Itkin, P., King, J., Merkouriadi, I., and Haapala, J.: A distributed snow‐evolution model for sea‐ice applications (SnowModel), Journal of Geophysical Research: Oceans, 123, 3786-3810, 2018.

Liu, C., Gao, Z., Yang, Q., Han, B., Wang, H., Hao, G., Zhao, J., You, L., Yang, Y., Wang, L., Li, Y.: Observed surface fluxes over sea ice near Antarctic Zhongshan station from April to November in 2016, Annals of Glaciology, 61(82) ,12-23, 2020.

Massonnet, F., Fichefet, T., Goosse, H., Vancoppenolle, M., Mathiot, P., and König Beatty, C.: On the influence of model physics on simulations of Arctic and Antarctic sea ice, The Cryosphere, 5, 687-699, 2011.

Maykut, G. A., and Untersteiner, N.: Some results from a time-dependent thermodynamic model of sea ice, Journal of Geophysical Research (1896-1977), 76, 1550-1575, 10.1029/JC076i006p01550, 1971.

McPhee, M. G., Kottmeier, C., and Morison, J. H.: Ocean Heat Flux in the Central Weddell Sea during Winter, J. Phys. Oceanogr., 29, 1166-1179, 10.1175/1520-0485(1999)029<1166:OHFITC>2.0.CO;2, 1999.

Merkouriadi, I., Liston, G. E., Graham, R. M., and Granskog, M. A.: Quantifying the potential for snow‐ice formation in the Arctic Ocean, Geophys. Res. Lett., 47, e2019G-e85020G, 2020.

Parkinson, C. L.: A 40-y record reveals gradual Antarctic sea ice increases followed by decreases at rates far exceeding the rates seen in the Arctic, Proceedings of the National Academy of Sciences, 116, 14414-14423, 2019.

Parkinson, C. L., and Cavalieri, D. J.: Antarctic sea ice variability and trends, 1979-2010, The Cryosphere, 6, 871-880, 2012.

Perovich, D. K., and Maykut, G. A.: Solar heating of a stratified ocean in the presence of a static ice cover, Journal of Geophysical Research: Oceans, 95, 18233-18245, 10.1029/JC095iC10p18233, 1990.

Provost, C., Sennéchael, N., Miguet, J., Itkin, P., Rösel, A., Koenig, Z., Villacieros Robineau, N., and Granskog, M. A.: Observations of flooding and snow‐ice formation in a thinner Arctic sea‐ice regime during the N‐ICE2015 campaign: Influence of basal ice melt and storms, Journal of Geophysical Research: Oceans, 122, 7115-7134, 2017.

Schlosser, E., Haumann, F. A., and Raphael, M. N.: Atmospheric influences on the anomalous 2016 Antarctic sea ice decay, The Cryosphere, 12, 1103-1119, 2018.

Stroeve, J. C., Serreze, M. C., Holland, M. M., Kay, J. E., Malanik, J., and Barrett, A. P.: The Arctic's rapidly shrinking sea ice cover: a research synthesis, Climatic Change, 110, 1005-1027, 2012.

Stuecker, M. F., Bitz, C. M., and Armour, K. C.: Conditions leading to the unprecedented low Antarctic sea ice extent during the 2016 austral spring season, Geophys. Res. Lett., 44, 9008-9019, 2017.

Tetzner, D., Thomas, E., and Allen, C.: A Validation of ERA5 Reanalysis Data in the Southern Antarctic Peninsula—Ellsworth Land Region, and Its Implications for Ice Core Studies, Geosciences, 9, 289, 2019.

Turner, A. K., Hunke, E. C., and Bitz, C. M.: Two modes of sea‐ice gravity drainage: A parameterization for large‐scale modeling, Journal of Geophysical Research: Oceans, 118, 2279-2294, 2013.

Turner, A. K., and Hunke, E. C.: Impacts of a mushy-layer thermodynamic approach in global sea-ice simulations using the CICE sea-ice model, Journal of Geophysical Research: Oceans, 120, 1253-1275, 2015.

Turner, J., Phillips, T., Marshall, G. J., Hosking, J. S., Pope, J. O., Bracegirdle, T. J., and Deb, P.:

https://doi.org/10.5194/tc-2021-134
Preprint. Discussion started: 17 June 2021

561 Unprecedented springtime retreat of Antarctic sea ice in 2016, Geophys. Res. Lett., 44, 6868-6875, 2017.
562 Uotila, P., Goosse, H., Haines, K., Chevallier, M., Barthélemy, A., Bricaud, C., Carton, J., Fučkar, N.,
563 Garric, G., and Iovino, D.: An assessment of ten ocean reanalyses in the polar regions, Clim. Dynam.,
564 52, 1613-1650, 2019.
565 Vancoppenolle, M., Timmermann, R., Ackley, S. F., Fichefet, T., Goosse, H., Heil, P., Leonard, K. C.,
566 Lieser, J., Nicolaus, M., and Papakyriakou, T.: Assessment of radiation forcing data sets for large-scale
567 sea ice models in the Southern Ocean, Deep Sea Research Part II: Topical Studies in Oceanography, 58,
568 1237-1249, 2011.
569 Vignon, É., Traullé, O., and Berne, A.: On the fine vertical structure of the low troposphere over the
570 coastal margins of East Antarctica, Atmos. Chem. Phys., 19, 4659-4683, 2019.
571 Wang, C., Graham, R. M., Wang, K., Gerland, S., and Granskog, M. A.: Comparison of ERA5 and ERA-
572 Interim near-surface air temperature, snowfall and precipitation over Arctic sea ice: effects on sea ice
573 thermodynamics and evolution, The Cryosphere, 13, 1661-1679, 2019b.
574 Wang, G., Hendon, H. H., Arblaster, J. M., Lim, E., Abhik, S., and van Rensch, P.: Compounding tropical
575 and stratospheric forcing of the record low Antarctic sea-ice in 2016, Nat. Commun., 10, 1-9, 2019a.
576 Wang, Y., Zhou, D., Bunde, A., and Havlin, S.: Testing reanalysis data sets in Antarctica: Trends,
577 persistence properties, and trend significance, Journal of Geophysical Research: Atmospheres, 121, 12-
578 839, 2016.
579 Yang, Q., Liu, J., Leppäranta, M., Sun, Q., Li, R., Zhang, L., Jung, T., Lei, R., Zhang, Z., and Li, M.:
580 Albedo of coastal landfast sea ice in Prydz Bay, Antarctica: Observations and parameterization, Adv.
581 Atmos. Sci., 33, 535-543, 2016a.
582 Yang, Y., Zhijun, L., Leppäranta, M., Cheng, B., Shi, L., and Lei, R.: Modelling the thickness of landfast
583 sea ice in Prydz Bay, East Antarctica, Antarct. Sci., 28, 59-70, 2016b.
584 Zhang, J.: Increasing Antarctic sea ice under warming atmospheric and oceanic conditions, J. Climate,
585 20, 2515-2529, 2007.
586 Zhang, J.: Modeling the impact of wind intensification on Antarctic sea ice volume, J. Climate, 27, 202-
587 214, 2014.
588 Zhao, J., Cheng, B., Yang, Q., Vihma, T., and Zhang, L.: Observations and modelling of first-year ice
589 growth and simultaneous second-year ice ablation in the Prydz Bay, East Antarctica, Ann. Glaciol., 58,
590 59-67, 2017.
591